

## Altered Structural and Mechanistic Properties of Mutant Dihydropteridine Reductases\*

(Received for publication, August 24, 1995, and in revised form, November 21, 1995)

Philip M. Kiefer‡, Kottayil I. Varughese‡§, Ying Su‡, Nguyen-H. Xuong‡, Chi-F. Chang§, Poonam Gupta§, Tom Bray§, and John M. Whiteley§¶

From the ‡University of California at San Diego, La Jolla, California 92093-0317 and §The Scripps Research Institute, La Jolla, California 92037

Nine single genetic mutants of rat dihydropteridine reductase (EC 1.6.99.7), D37I, W86I, Y146F, Y146H, K150Q, K150I, K150M, N186A, and A133S and one double mutant, Y146F/K150Q, have been engineered, overexpressed in *Escherichia coli* and their proteins purified. Of these, five, W86I, Y146F, Y146H, Y146F/K150Q, and A133S, have been crystallized and structurally characterized. Kinetic constants for each of the mutant enzyme forms, except N186A, which was too unstable to isolate in a homogeneous form, have been derived and in the five instances where structures are available the altered activities have been interpreted by correlation with these structures. It is readily apparent that specific interactions of the apoenzyme with the cofactor, NADH, are vital to the integrity of the total protein tertiary structure and that the generation of the active site requires bound cofactor in addition to a suitably placed W86. Thus when the three major centers for hydrogen bonding to the cofactor are mutated, *i.e.* 37, 150, and 186, an unstable partially active enzyme is formed. It is also apparent that tyrosine 146 is vital to the activity of the enzyme, as the Y146F mutant is almost inactive having only 1.1% of wild-type activity. However, when an additional mutation, K150Q, is made, the rearrangement of water molecules in the vicinity of Lys<sup>150</sup> is accompanied by the recovery of 50% of the wild-type activity. It is suggested that the involvement of a water molecule compensates for the loss of the tyrosyl hydroxyl group. The difference between tyrosine and histidine groups at 146 is seen in the comparably unfavorable geometry of hydrogen bonds exhibited by the latter to the substrate, reducing the activity to 15% of the wild type. The mutant A133S shows little alteration in activity; however, its hydroxyl substituent contributes to the active site by providing a possible additional proton sink. This is of little value to dihydropteridine reductase but may be significant in the sequentially analogous short chain dehydrogenases/reductases, where a serine is the amino acid of choice for this position.

The regeneration of the tetrahydrobiopterin cofactor that participates in the initial hydroxylation reactions of the aromatic amino acids, phenylalanine, tryptophan, and tyrosine, essential for the generation of the catecholamines (1–4), is carried out by the NADH-requiring enzyme, dihydropteridine reductase (EC 1.6.99.7). Recent reports from this laboratory have described the crystal structures of this enzyme derived from both rat and human sources (5, 6), have identified its classification into the larger protein families of the short chain dehydrogenases (7) and epimerases (8, 9), and have suggested that the Tyr-(Xaa)<sub>3</sub>-Lys-containing motif is essential to the reductive mechanism of the protein (10).

During the course of this investigation, it has become apparent that certain amino acids are essential to the binding of the dinucleotide cofactor. Of particular importance are Asp<sup>37</sup>, Lys<sup>150</sup>, and Asn<sup>186</sup>, as each of these amino acids display strong hydrogen bonds to the adenine ribose, nicotinamide ribose, and nicotinamide amide substituent, respectively. In addition, Tyr<sup>146</sup> interacts with both Lys<sup>150</sup> and the 4-position of the quinonoid dihydrobiopterin substrate placed by graphic computations at the ternary complex active site. Moreover, Trp<sup>86</sup> appears to orient the plane of the pteridine by steric interactions. It is also apparent that when a sequence comparison is made between dihydropteridine reductase and the family of short chain dehydrogenases/reductases, in the majority of cases Ala<sup>133</sup> is converted to Ser (11). We describe here the altered properties of dihydropteridine reductase when Lys<sup>150</sup> is replaced with Gln, Ile, and Met, when Tyr<sup>146</sup> is replaced by Phe and His, when a double mutant Tyr<sup>146</sup> → Phe/Lys<sup>150</sup> → Glu is generated, when Trp<sup>86</sup> is converted to Ile and when Asn<sup>186</sup> is converted to alanine. In addition an Ala<sup>133</sup> → Ser variant of dihydropteridine reductase has been created to help discover if the prevalence for this change in the dehydrogenases can be interpreted. Crystal structures of several of the mutants have been obtained and structural changes occurring in these derivatives have been used to interpret the altered kinetic properties of the mutated enzymes. Together, these results support the concept that the dihydropteridine reductase protein requires a tightly bound reduced dinucleotide for structural and mechanistic integrity and that the Tyr-(Xaa)<sub>3</sub>-Lys motif is important to the proton transfer that may initiate or complete substrate reduction.

### EXPERIMENTAL PROCEDURES

**Materials**—Oligonucleotide syntheses were carried out with an automated Applied Biosystems synthesizer at this institute (The Scripps Research Institute). The gene for the wild-type rat dihydropteridine reductase was contained in the plasmid pKQV4, which was constructed as described previously (12). Expression of the plasmid was in the DH5α strain of *Escherichia coli* obtained from Life Technologies, Inc. Restriction enzymes *Eco*RI and *Hind*III were obtained from New England Biolabs. The general methods of ligation, transformation of *E. coli*, and screening of clones by restriction analysis were performed as described

\* This investigation was supported in part by Grants CA11778 and GM52699 from the National Institutes of Health and the Sam and Rose Stein Charitable Trust (TSRI) and Grants RR01644, DK44125, and HmG00005 (Human Genome Training Grant) from the National Institutes of Health, Grant DIR88–22385 from the National Science Foundation, and the Lucille P. Markey Foundation (University of California, San Diego). This is publication number 9435-MEM from the Department of Molecular and Experimental Medicine at The Scripps Research Institute. The costs of publication of this article were defrayed in part by the payment of page charges. This article must therefore be hereby marked “advertisement” in accordance with 18 U.S.C. Section 1734 solely to indicate this fact.

¶ To whom correspondence should be addressed: Dept. of Molecular & Experimental Medicine, NX 2, The Scripps Research Institute, 10666 North Torrey Pines Rd., La Jolla, CA 92037. Tel.: 619-784-7910; Fax: 619-784-7981.

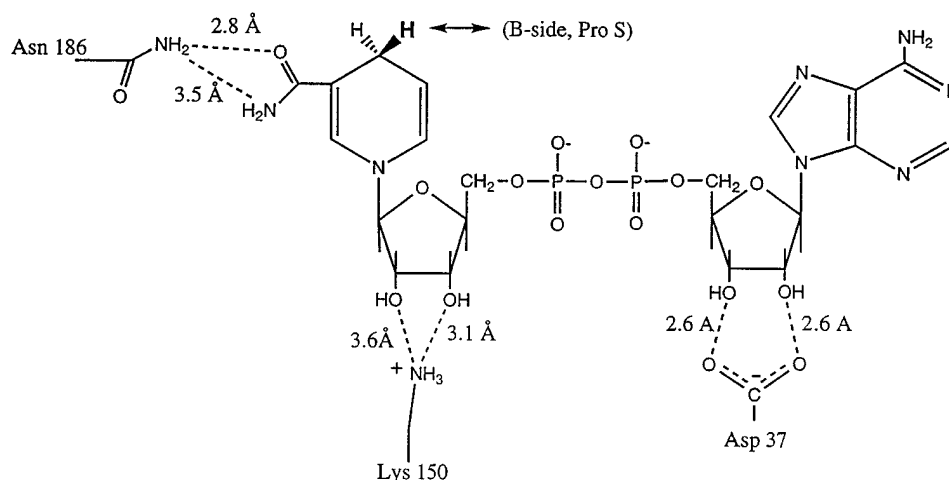


FIG. 1. The structure of the reduced dinucleotide NADH showing the pertinent interactions with Asp<sup>37</sup>, Lys<sup>150</sup>, and Asn<sup>186</sup> and the measured bond lengths derived from the crystal structure of the binary complex with the *E. coli* expressed rat dihydropteridine reductase.

elsewhere (13–15). Final verification of plasmid clones and constructs was achieved by dideoxy DNA sequencing using the Sequenase kit from U. S. Biochemical Corp. Site-directed mutagenesis employed uracil-enriched single-stranded plasmid DNA obtained from a Bio-Rad Mutagenesis M13 *in vitro* mutagenesis kit based on procedures described by Kunkel (16, 17). The following oligonucleotides were used to promote mutant formation: Ala<sup>133</sup> → Ser, ACC CTG GCC GGG TCT AAA GCT GCGTTG; Lys<sup>150</sup> → Glu, GGC TAC GGC ATG GCC CAG GGA CGG CTC CAT CAG; Lys<sup>150</sup> → Ile, GGC ATG GCC ATC GAA GCC GTC CAT; Lys<sup>150</sup> → Met, GGC ATG GGC ATG GGA GCC GTC CAT; Tyr<sup>146</sup> → Phe, GGG ATG ATT GGC TTC GGC ATG GCC AAG; Tyr<sup>146</sup> → His, GGG ATG ATT GGC CAC GGC ATG GCC; Tyr<sup>146</sup> → Phe/Lys<sup>150</sup> → Gln, a composite of the single mutation sequences; Trp<sup>86</sup> → Ile GTG GCT GGA GGA ATC GCC GGG GGC AAT and Asn<sup>186</sup> → Ala, GAT ACT CCG ATG GCT AGG AAA TCA ATG. 2-Amino-4-hydroxy-6,7-dimethyl-5,6,7,8-tetrahydropteridine was obtained from Sigma, (6*R*)-L-erythro-5,6,7,8-tetrahydrobiopterin from Dr. B. Schircks Laboratories (Jona, Switzerland), and isopropyl-1-thio-β-D-galactopyranoside from Diagnostic Chemicals Ltd. (Charlottetown, Canada). Unless stated otherwise, bacteria were grown in LB medium containing 50–100 μg/ml ampicillin with shaking at 37 °C.

**Protein Purification**—In a typical preparation, 10 liters of cells in LB medium were grown to  $A_{600\text{ nm}} = 0.6\text{--}0.7$  (~3 h after inoculation) at 37 °C and then induced to express mutant or wild-type dihydropteridine reductase with 1 to 2 mM IPTG. After a further 2 h they were combined and centrifuged at  $8000 \times g$  for 10 min. The pellets were resuspended in a minimal volume of 0.1 M potassium phosphate, pH 6.8, containing 0.001 M β-mercaptoethanol (present in all subsequent buffer solutions) and 20 μM TPCK, TLCK and PMSF, then centrifuged at  $8000 \times g$  for 10 min. The pellets were then taken up in the least quantity of 0.01 M acetic acid again containing 20 μM protease inhibitors and sonicated on ice for  $5 \times 15$  s. The homogenate was centrifuged at  $10,000 \times g$  for 45 min and the combined supernatant treated with  $(\text{NH}_4)_2\text{SO}_4$ . The 20–41% fraction was collected by centrifugation and redissolved in 0.05 M potassium phosphate, pH 6.8. Following extensive dialysis against this same buffer solution the material was applied to two consecutive columns of Cibacron blue agarose (Pharmacia Biotech, Inc.). In the former, elution was achieved with a NaCl gradient and in the latter with NADH as has been described previously (12). A final purification step was achieved by passage through Sephacryl (Sigma). In this step it was necessary to ensure concentrations of 10–100 mM NADH were present in the standard eluting buffer for mutants whose affinity for NADH was reduced. At this stage the protein was usually homogenous by SDS-PAGE. Yields were ~10–15 mg from a 10-liter preparation. Usually 0.5–1.0 ml of a solution of protein containing 10 mg/ml was required for crystallography.

**Assay**—Dihydropteridine reductase initial velocities were obtained spectrophotometrically according to the procedure of Webber *et al.* (18), and protein concentrations were obtained by Bradford determinations (19). Elimination of trace impurities and isolation of apoenzyme by HPLC, SDS-PAGE, kinetic measurements, and fluorescence measurements of NADH dissociation constants were all measured by procedures outlined in detail in Ref. 12.

**X-ray Crystallography**—Crystals of binary complexes with NADH were grown by a hanging drop vapor diffusion method using conditions similar to those in which the original rat liver source enzyme was crystallized (20). Crystals were obtained at 4 °C using polyethylene glycol 4500 as a precipitant with various concentrations of Tris phosphate, pH 7.8, containing 10% (v/v) methanol. Measurements were obtained from graphite-monochromated CuK α radiation ( $D = 1.5418$  Å) with the use of a multiwire area detector system (21) at the University of California at San Diego, Research Resource. The structures were solved by difference Fourier techniques with standard refinement procedures employing X-PLOR (22) and using the native dihydropteridine reductase structure (5). The verification of the mutated residues was done with the combination of rigidly body refinement, omit maps, and difference maps calculated by X-PLOR and displayed by FRODO (23). Difference maps also defined water positions in the mutants for comparison with the established native water positions. Only water molecules in or around the active site were built into the structures. In this report crystal structures of Ala<sup>133</sup> → Ser, Tyr<sup>146</sup> → Phe, Tyr<sup>146</sup> → His, Tyr<sup>146</sup> → Phe/Lys<sup>150</sup> → Gln, and Trp<sup>86</sup> → Ile are described.

**Model for the Ternary Complex**—Quinonoid dihydrobiopterin was positioned in the active site of the wild-type and mutant binary complexes according to previously described procedures with movement restricted by the parameter that N5 of the pteridine molecule is ~3.3 Å from C4 of the nicotinamide component of NADH. The distance constraint of 3.3 Å mimics the NADH binding interaction of glutathione reductase (24), dihydrofolate reductase (25), and model hydride transfer compounds (26). The substrate stacks between the nicotinamide and Trp<sup>86</sup> with the pteridine ring parallel to the plane of the nicotinamide ring. The best geometrical fit that avoids steric interactions has the re-face of the pteridine ring rotated above the nicotinamide with the dihydroxypropyl 6-substituent pointing away from the nicotinamide ring (5). This model forms the basis for the structural and mechanistic explanations of the comparative properties of the mutant proteins described in this report.

## RESULTS

Examination of the binary complex of dihydropteridine reductase and NADH (5) indicates that the principal hydrogen bonding protein interactions occur between the dinucleotide and Asp<sup>37</sup>, Lys<sup>150</sup>, and Asn<sup>186</sup> (Fig. 1). In order to estimate the importance of each of these sites, they have been mutated to afford differing proteins containing Asp<sup>37</sup> → Ile (27), Lys<sup>150</sup> → Gln, Lys<sup>150</sup> → Ile, Lys<sup>150</sup> → Met, and Asn<sup>186</sup> → Ala amino acid changes. If the ternary complex employing a graphically introduced quinonoid dihydrobiopterin substrate is also analyzed (5), a further site of interaction appears between substrate and Tyr<sup>146</sup>. Mutations of this site to Phe or His have also been carried out and each gives rise to a protein with significantly altered enzymatic properties. In addition, the planar Trp<sup>86</sup> has been replaced by Ile to discover the former's influence on the

TABLE I  
Kinetic constants for *E. coli* expressed wild-type and mutant forms of the rat dihydropteridine reductase

Enzyme	$K_m$ , [qPtH <sub>2</sub> ] <sup>a</sup>	$K_m$ , [NADH]	$k_{cat}$	$K_d$ , [NADH]	Comparative activity
	$\mu M$	$\mu M$	$s^{-1}$	$\mu M$	%
Wild-type	27	13	153 <sup>b</sup>	0.024	100
Asp <sup>37</sup> → Ile <sup>c</sup>	30	36	36	0.35	23
Trp <sup>86</sup> → Ile	70	12	64	0.030	42
Tyr <sup>146</sup> → Phe	0.9 <sup>d</sup>	10	1.7	0.091	1.1
Tyr <sup>146</sup> → His	23	17	23	0.041	15
Tyr <sup>146</sup> → Phe/Lys <sup>150</sup> → Gln	41	27	76	0.28	50
Lys <sup>150</sup> → Gln	33	29	90	0.17	59
Lys <sup>150</sup> → Ile	26	21	64	0.20	42
Lys <sup>150</sup> → Met	39		26	0.35	17
Asn <sup>186</sup> → Ala	Unstable				
Ala <sup>133</sup> → Ser	20	25	149	0.055	97

<sup>a</sup> qPtH<sub>2</sub>, quinonoid dihydrobiopterin.

<sup>b</sup> The  $k_{cat}$  values are from measurements taken at fixed pteridine concentrations. An approximate molecular weight of 51,000 is used for dihydropteridine reductase in the calculation (cf.  $M_r$  (rat) = 50,849 (38)).

<sup>c</sup> Taken from Ref. 27.

<sup>d</sup> The high concentration of protein necessary to secure measureable reaction rates could introduce a larger error into this figure.

active site. Since sequential comparisons have indicated dihydropteridine reductase is a member of the class of proteins known as short chain dehydrogenases (11), it can also be deduced that Ala<sup>133</sup> could have some influence on the structural properties of the reductase as this amino acid is usually a serine in the dehydrogenases. Therefore, the Ala<sup>133</sup> → Ser mutant has also been created. Each of the mutations influences the structural and kinetic properties of dihydropteridine reductase and the latter are illustrated in Table I.

The crystal data and refinement statistics for all mutants are given in Table II. All mutant crystals were similar in form to the native: orthorhombic C222<sub>1</sub> with  $a = 50.10$  Å,  $b = 139.13$  Å, and  $c = 64.93$  Å. Structures were refined to an  $R \leq 18\%$ . There was very little overall structural change between the native and mutant proteins; however, significant changes occurred around the particular amino acid that was mutated. In particular, a difference of bound water molecules was noted in the active site.

It was necessary to devise a series of omit maps for the various mutants in order to confirm that the specific insertions had occurred and to measure the changes in electron density associated with the replacement amino acids.

**Tyr<sup>146</sup> → Phe**—Fig. 2a shows the difference map of the native structure including a tyrosine at site 146. The large negative peak in this figure corresponds to the omission of hydroxyl density consistent with the presence of a phenylalanine at 146. Fig. 2b illustrates the 2.5 $\sigma$  difference map of the wild-type enzyme structure omitting the side chain of residue 146 computed with the Tyr<sup>146</sup> → Phe data. The positive density in Fig. 2b is supportive of the presence of a Phe at 146. Moreover, a difference Fourier map also indicates a significant shift of water molecule 320. In the native enzyme, this water molecule is hydrogen bonded to the hydroxyl of Tyr<sup>146</sup>, whereas the lack of the tyrosyl hydroxyl group in the phenylalanine replacement residue of the mutant has this water primarily hydrogen bonding to the nicotinamide ribose hydroxyl group.

**Tyr<sup>146</sup> → Phe/Lys<sup>150</sup>Gln**—Difference maps similar to those obtained for the single Tyr<sup>146</sup> → Phe mutant also support the presence of a phenylalanine at 146 with the double mutant. A further omit difference map was computed excluding the side chains of 146 and 150 after rigid body refinement. Fig. 2c is the omit difference map in the region of the side chain of residue 150. Electron density occurs in a dual asymmetric lobe for the 150 side chain, supporting a glutamine residue. However, the distinction between the amino group and the carbonyl oxygen of glutamine is yet to be determined. The extra density in one of the lobes would imply this atom could be an oxygen hydro-

gen-bonded to Ser<sup>107</sup> (cf. Fig. 4). The preferred hydrogen bond of glutamine with Ser<sup>107</sup> would be toward the carbonyl oxygen. Refinement and slow cooling methods have shown this to be a favored configuration. The change from lysine to glutamine at position 150 allows an extra water molecule site at a distance  $\sim 4$  Å to both the amido oxygen and nitrogen of Gln 150 (cf. Fig. 4). In addition, the double mutant has H<sub>2</sub>O 320 in a similar position to that of the single Tyr<sup>146</sup> → Phe mutant.

**Tyr<sup>146</sup> → His**—In the Tyr<sup>146</sup> → His mutant, a difference in electron density can be observed for the side chain of residue 146. A difference map between the native structure and the Tyr<sup>146</sup> → His data shows a large negative peak similar to that in Fig. 2a, indicating the lack of a tyrosyl oxygen. A difference map computed with the Tyr<sup>146</sup> → His data and a native structure that omits the side chain from residue 146 confirms a histidine is present (Fig. 2d) and in addition shows the lack of water molecule 320.

**Trp<sup>86</sup> → Ile**—This difference map (Fig. 2e) omits the side chain of residue 86. The map clearly shows the density of isoleucine, a much smaller residue than tryptophan. In this instance H<sub>2</sub>O 320 hydrogen-bonds with the ribose hydroxyl group of the nicotinamide and not with the hydroxyl group of Tyr<sup>146</sup> as was shown with the wild-type enzyme.

**Ala<sup>133</sup> → Ser**—Fig. 2f shows the map comparing the A133S data with that of the native structure. A large positive peak is seen in the vicinity of the C $\beta$  of Ala<sup>133</sup> corresponding to the OH of serine. An additional difference in this region is the absence of water molecule 263. In the native and other mutant structures H<sub>2</sub>O 263 forms hydrogen bonds with the backbone nitrogen atoms of amino acids 134 and 135 and the backbone oxygen of amino acid 178 forming a tight loop. In contrast, in this mutant the hydroxyl group of Ser<sup>133</sup> appears to substitute for H<sub>2</sub>O 263. It is interesting to note that Ser<sup>133</sup> in dihydropteridine reductase is in a comparable position with that of Ser<sup>139</sup> in the 3 $\alpha$ ,20 $\beta$ -hydroxysteroid dehydrogenase; a typical member of the class of short chain dehydrogenases whose structure has been reported (28). It is also apparent that H<sub>2</sub>O 320 is at the position seen in other mutants.

As was described earlier (27), Asp<sup>37</sup> resides at the end of a typical Rossman fold that exhibits close affinity for the adenine ribose component of NADH. The crystal structure of the native enzyme shows strong hydrogen bonds between the distal aspartate carboxyl and the 2'- and 3'-hydroxyl groups of the ribose unit (Fig. 1). Consistent with the loss of these hydrogen bonds in the Asp<sup>37</sup> → Ile mutant is the lower affinity exhibited by this mutant compared to wild type for NADH ( $K_d = 0.35$   $\mu M$  compared with  $K_d = 0.024$   $\mu M$ ). Clearly this is an order of

TABLE II  
X-ray crystallographic data and statistics for the five orthorhombic ( $C222_1$ ) mutant dihydropteridine reductase (DHPR) structures: Y146F, Y146H, A133S, W86I, and Y146F/K150Q

DHPR mutant	Unit cell dimensions			Resolution	$R_{\text{sym}}^a$	Observations	Unique reflections	Completeness	$I/\sigma$ at outer shell	Final $R$ factor at 2.3 Å	rms dev. bond lengths	rms dev. bond angles
	$a$	$b$	$c$									
	Å			Å	%			%		%	Å	degrees
Y146F	50.25	139.31	64.91	2.1	6.9	91,417	14,858	99.0	4.8	17.5	0.011	1.7
Y146H	50.13	139.06	64.83	2.3	8.0	31,047	10,464	94.5	1.9	17.6	0.013	1.9
A133S	50.19	139.19	64.78	2.2	8.4	72,702	12,213	91.4	2.7	18.0	0.012	1.8
W86I	50.14	139.20	64.90	2.3	5.6	43,581	10,164	94.0	3.5	17.5	0.011	1.7
Y146F/K150Q	50.21	138.90	64.93	2.3	6.9	46,925	10,476	97.5	2.4	17.0	0.012	1.8

<sup>a</sup>  $R_{\text{sym}} = \sum_h \sum_{i=1}^N |I(h) - \bar{I}(h)| / \sum_h \sum_{i=1}^N I(h)_i$ , where  $I(h)_i$  is the  $i$ th measurement of reflection  $h$  and  $\bar{I}(h)$  is the mean value of the  $N$  equivalent reflections.

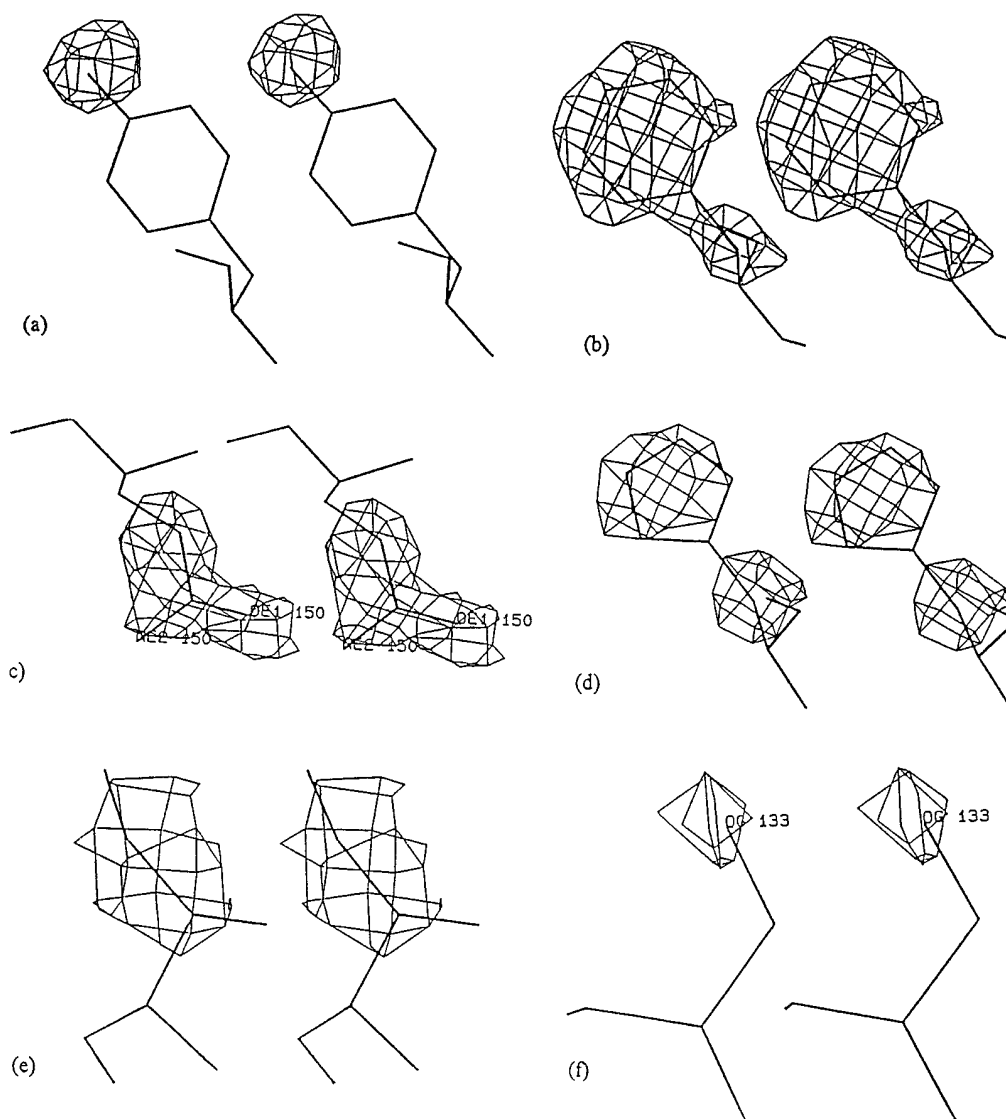


FIG. 2. *a* and *f* are difference maps computed with the mutant diffraction data and the wild-type coordinates. *b*–*e* are omit maps computed excluding the appropriate side chains from the wild-type model. *a*, Y146F difference map. *b*, Y146F omit map. *c*, Y146F/K150Q omit map at residue 150. *d*, Y146H omit map. *e*, W86I omit map. *f*, A133S difference map. Contours are drawn at  $3\sigma$  (*c*, *e*, and *f*),  $-3\sigma$  (*a*) and  $2.5\sigma$  (*b* and *d*) levels.

magnitude transition with an associated significant fall off in  $k_{\text{cat}}$  to  $36\text{ s}^{-1}$ , demonstrating only 23% of the wild-type activity. Progressing along the NADH molecule, from *right to left* in Fig. 1, Lys<sup>150</sup> interacts with the nicotinamide ribose. Mutations to Gln, Ile, and Met demonstrate the importance of this linkage and  $K_d$  values from 0.17 to  $0.35\text{ }\mu\text{M}$  were measured and  $k_{\text{cat}}$  values from 59 to 17% of wild type. A final important interaction occurs between Asn<sup>186</sup> and the carboxamide of the nicotinamide. The conversion of this amino acid to alanine in dihy-

dropteridine reductase explores this feature. So far this mutant has proven too unstable to purify.

Because of difficulties associated with the practical isolation and crystallization of a dihydropteridine reductase ternary complex, the issue has been resolved by the graphical introduction of quinonoid dihydrobiopterin into the active site (25). This model is based on the premise that the N5 position of the pteridine is the recipient of the hydride transfer from NADH (29, 30) and the probability that C4 of the nicotinamide and N5

FIG. 3. The pH profiles of enzymatic activity. All mutants, except Tyr<sup>146</sup> → His, have the general profile illustrated for the wild-type enzyme (A) (●). Tyr<sup>146</sup> → His is shown on the same scale (▲) and enlarged in B (▲).

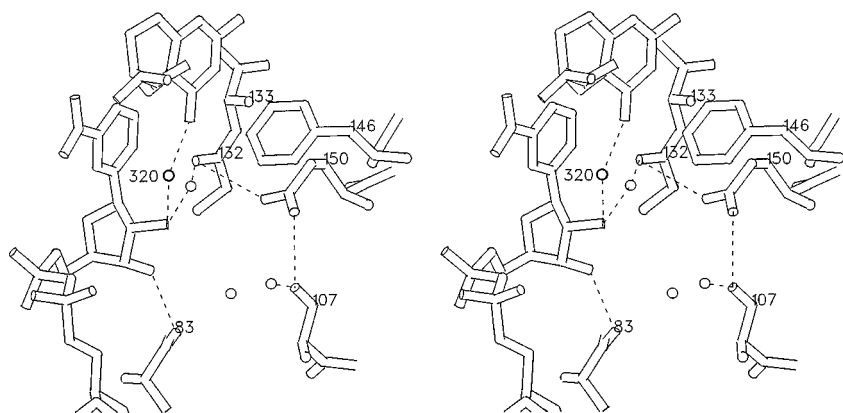
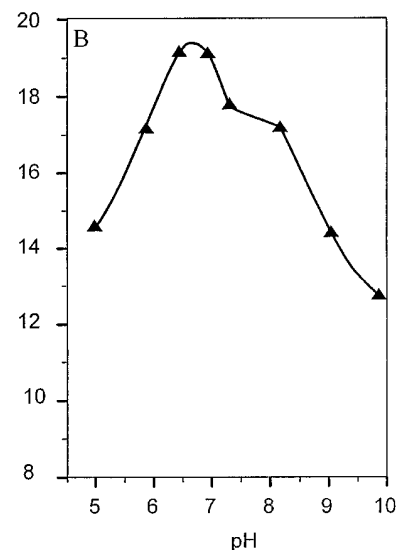
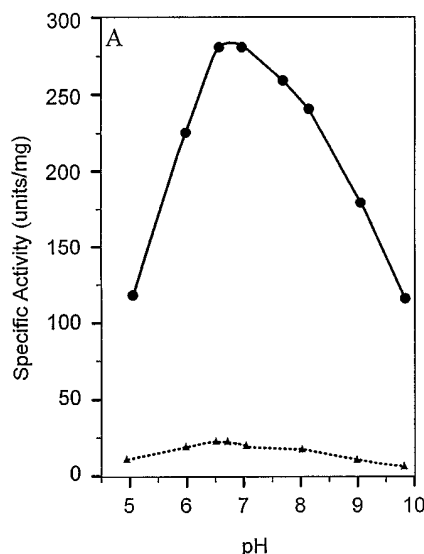


FIG. 4. Stereoview of the Tyr<sup>146</sup> → Phe/Lys<sup>150</sup> → Gln mutant active site showing bound pteridine and NADH and the hydrogen bonding network around glutamine 150. Water molecule 320 is clearly shown hydrogen bonded to both pteridine and ribose 2' hydroxyl groups, with Gln<sup>150</sup> in the mutant somewhat more distant from the NADH than Lys<sup>150</sup> in the wild-type structure. Water molecule 320 and selected amino acids are numbered. Potential sites for hydrogen bonding are illustrated by broken lines.

of the pteridine are within 3.3 Å of each other (5). When these restrictions are applied it is apparent from crystal structure data that Tyr<sup>146</sup> is within hydrogen bonding distance of the C4 oxygen of the pteridine. Previously it has been hypothesized that tyrosine might be the compensatory proton donor for the hydride transfer from the reduced dinucleotide (10), therefore mutation of this amino acid to phenylalanine should have serious consequences for the enzyme. In fact  $k_{\text{cat}}$  drops to 1.1% of the wild-type value when this change is introduced. Interestingly, the  $K_d$  for NADH is only marginally altered and  $K_m$  values for both substrates, although lower, probably contain a greater error factor that reflects the difficulty of measuring the low specific activity exhibited by the protein by the usual assay. The second of these mutations Tyr<sup>146</sup> → His is somewhat more active as might be expected *a priori* as histidine can itself be a proton donor.  $k_{\text{cat}}$  rises to 15% of wild type,  $K_m$  values for both substrates are normal, and the  $K_d$  for NADH is virtually that of wild type. Mutation of Trp<sup>86</sup> to Ile removes the large planar steric interaction that sandwiches the substrate in the active site and the kinetic results alter accordingly. The  $K_d$  for NADH is unaltered, but the  $k_{\text{cat}}$  falls to 42% of wild-type and the  $K_m$  for the pteridine substrate rises to twice the usual figure.

Surprisingly, the double mutant Tyr<sup>146</sup> → Phe/Lys<sup>150</sup> → Gln gives a considerable rise in  $k_{\text{cat}}$  to 50% of the wild-type rate when compared with the Tyr<sup>146</sup> → Phe mutant alone. The  $K_d$  for NADH in this mutant is comparable with that of the Lys<sup>150</sup> → Gln single mutant and  $K_m$  values for both substrates are little altered. The Ala<sup>133</sup> → Ser mutation gave no unusual results for this enzyme. The  $k_{\text{cat}}$  was 97% of wild type, the  $K_d$  for NADH was marginally altered and the  $K_m$  values for both

substrates were similar to the wild type.

The pH activity profiles for each of the mutants except, Tyr<sup>146</sup> → His, were similar having a single peak of activity at approximately 7 with lower rates toward higher and lower pH values (Fig. 3). Using the standard assay, results lose their accuracy below pH 6 because of the high rate of acid catalyzed NADH decomposition and at greater than 10 because of an erratic blank rate probably caused by quinonoid dihydropteridine decomposition. Only the Tyr<sup>146</sup> → His mutant shows an altered profile. A clear shoulder appears at pH 8.5 in addition to the peak of activity at pH 7.

#### DISCUSSION

Of the many mutants examined kinetically, five have been crystallized and structurally characterized: Trp<sup>86</sup> → Ile, Tyr<sup>146</sup> → His, Tyr<sup>146</sup> → Phe, Tyr<sup>146</sup> → Phe/Lys<sup>150</sup> → Gln, and Ala<sup>133</sup> → Ser. Asp<sup>37</sup> → Ile, the various single mutants at 150, and Asn<sup>186</sup> → Ala proved extremely unstable to purification. When in the presence of a 5–10-fold molar excess of NADH they remained stable at low temperature in solution. Unfortunately, low yields ensued from chromatography unless buffer solutions contained very high concentrations of the dinucleotide, making the practical necessity of repeated purifications prohibitively expensive. Nevertheless, sufficient quantities of the Lys<sup>150</sup> → Gln, Lys<sup>150</sup> → Ile, and Lys<sup>150</sup> → Met, but not the Asn<sup>186</sup> → Ala mutants were isolated for rapid measurements of kinetic constants. Activity was lost, however, too rapidly for the isolation of sufficient purified material to allow x-ray crystallography. This observation suggests the hydrogen bonds connecting Asp<sup>37</sup>, Lys<sup>150</sup>, and Asn<sup>186</sup> to the two ribose components and

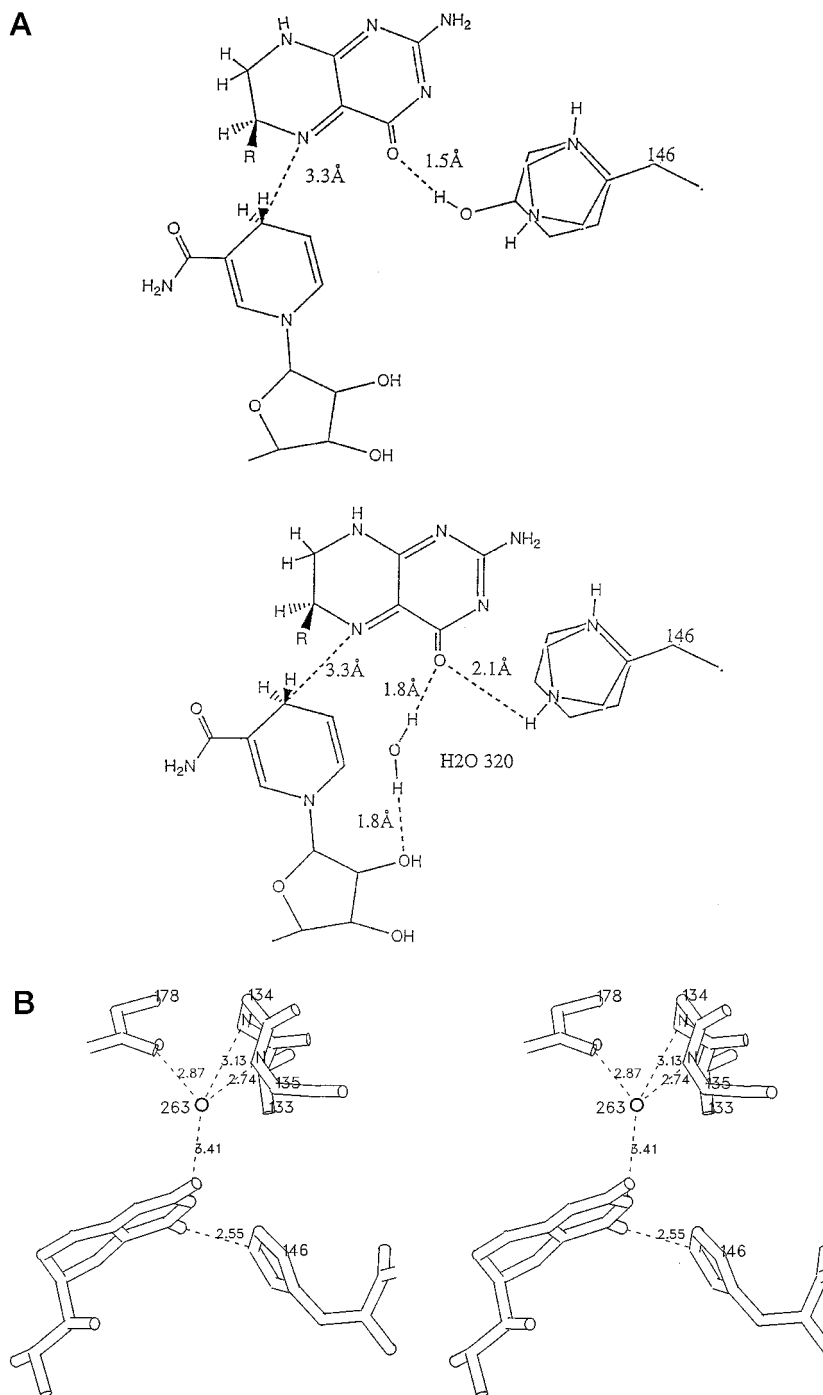


FIG. 5. A, scheme illustrating the unfavorable hydrogen bonding interaction between pteridine substrate and histidine 146 in the Y146H mutant. *R* is the dihydroxypropyl substituent of biopterin. *Top*, wild-type model substrate interactions with the His of the Tyr<sup>146</sup> → His mutant superimposed. *Bottom*, model substrate interaction comparing Phe and His at 146. With Phe at 146, H<sub>2</sub>O 320 is present, but with the His mutant this water molecule is not present at this position. B, stereoview of the hydrogen bonding network associated with water molecule 263 that could offer alternate proton sources for completion of the reductive process. Nomenclature is as described in the legend to Fig. 4 with additional selected nitrogen and oxygen sites on the protein backbone being emphasized for clarity and hydrogen bond lengths marked in Å.

carboxamide of the dinucleotide (Fig. 1) are of prime importance for securing the correct orientation and binding of NADH to the protein backbone.

The loss of activity exhibited by the single mutant Tyr<sup>146</sup> → Phe has been attributed to the loss of the phenolic tyrosine OH. Structural alignment of Tyr<sup>146</sup> and Lys<sup>150</sup> suggest interactive forces might exist of sufficient magnitude to allow liberation of the phenolic hydrogen as a proton and thus provide the compensatory proton transfer required to match the NADH hydride donation occurring to the pteridine in the reductive process (10). Analogous transfers have been suggested in the case of aldose reductase (31) and the dehydrogenases (32).

Surprisingly, the double mutant Tyr<sup>146</sup> → Phe/Lys<sup>150</sup> → Gln was also sufficiently stable to allow purification and crystallization (Fig. 4). This is difficult to understand as the Lys<sup>150</sup> → Gln change might suggest similar instability to the single mu-

tant would occur. Probably, the introduction of the second mutant, Tyr<sup>146</sup> → Phe, must alter the orientation of the various functional groups in this region of the molecule. This conclusion for the enhanced double mutant binary complex stability is supported by the observation that loss of the phenolic OH of the tyrosine in the single Tyr<sup>146</sup> → Phe mutant causes a profound 2 orders of magnitude change in  $k_{\text{cat}}$  (Table I), whereas, in contrast, the double mutant regains considerable activity to give up to 50% of the wild-type response. Examination of the active site of the double mutant (Fig. 4) suggests that the altered position taken by H<sub>2</sub>O 320 might be a major contributor to both the enhanced stability and increased activity of the double mutants. Upon substrate binding, this water molecule is in a position to hydrogen-bond with the carbonyl O4 of the pterin and thus is capable of transferring a proton to the substrate. It is of interest that this water molecule 320 is

FIG. 6. Stereoview of the Trp<sup>86</sup> → Ile mutant structure showing the altered interaction of this amino acid side chain with the pteridine substrate. For comparison, the wild-type structure has been superimposed at this position. The nomenclature is as described in the legend to Fig. 5.

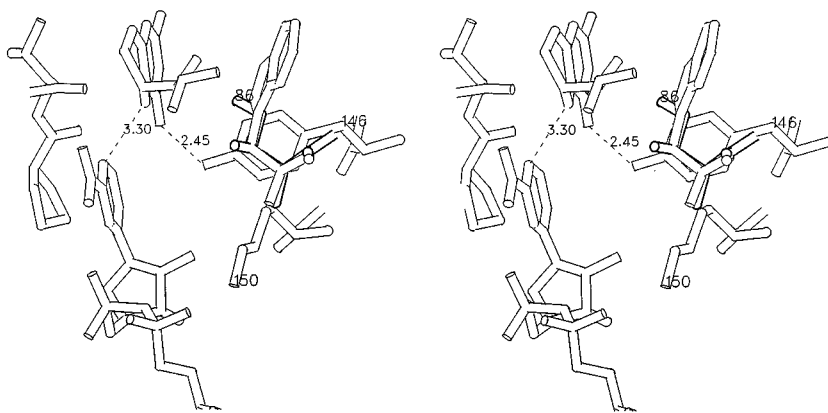
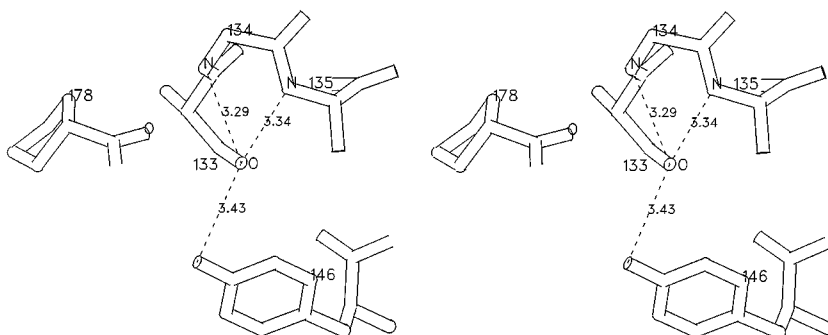


FIG. 7. Stereoview of the Ala<sup>133</sup> → Ser mutant structure showing the hydrogen bonding network created when a serine is introduced at this position. Also shown are additional interactions created to the backbone of amino acids 134 and 135. The nomenclature is as described in the legend to Fig. 5b.



present in a similar position in all of the mutants except Tyr<sup>146</sup> → His. In each case, the water is bound to the nicotinamide ribose hydroxyl. The B-factor for the H<sub>2</sub>O 320 site is ~30 Å<sup>2</sup>, except in the case of the double mutant, in which it has a B-factor of ~10 Å<sup>2</sup>. In Tyr<sup>146</sup> → Phe, only half occupancy gives H<sub>2</sub>O 320 a B-factor of ~10 Å<sup>2</sup>. This suggests that the substitution of a lysine by a glutamine in the double mutant causes a local environmental change in which water is bound more strongly. This apparent increase in stability of this water molecule appears significant as it is correlated with the recovery of activity by the Tyr<sup>146</sup> → Phe/Lys<sup>150</sup> → Gln double mutant.

When Tyr<sup>146</sup> is replaced by a histidine, only a 2-fold higher change in  $K_d$  is observed for NADH, relative to wild type; however, there is a considerable loss of activity (*i.e.* ~85%). This probably reflects the change of proton donor from tyrosine to histidine. Although, histidine should be a better proton donor, the hydrogen bond geometry with tyrosine and histidine at the active site is different. As seen in Fig. 5, the substrate can bind in a position such that the O4 of the substrate forms a hydrogen bond with the histidine, but the angle of proton transfer is less than ideal. Moreover, the histidine interaction could be more complex. Just as the pK of the tyrosine proton is affected by the proximity of the protonated amino group of lysine 150, so could the protonation of the histidine imidazole be affected. In addition, it is apparent in Fig. 5 that the 2-amino substituent and 3-nitrogen of the quinonoid dihydrobiopterin substrate are near water molecule 263. The delocalization of the quinonoid pteridine electronic structure is such that the compensatory protonation to hydride transfer could occur at the 2-, 3-, or 4-positions (33). Therefore, in the case of the histidine mutant, this altered reaction pathway might occur to afford the 15% residual activity and may also contribute to the altered pH profile shown in Fig. 3. The water molecule 263 is present in all the other structures, except the Ala<sup>133</sup> → Ser mutant, but it would appear that in these instances protonation is favored to occur from the tyrosine hydroxyl or its aqueous replacement. It is not inconceivable a minimal contribution

from this alternate proton source might occur with other mutants. It is interesting to note that when the tyrosine proton donor occurring at the active site of aldose reductase is replaced by histidine, compensatory movements of molecular water are observed (31).

It is apparent from the orientation of Trp<sup>86</sup> relative to the active site (5) that considerable interaction is possible between this planar substituent and the planar pteridine substrate. The tryptophan side chain keeps the substrate pinned against the nicotinamide ring. It is therefore not surprising that the generation of the Trp<sup>86</sup> → Ile mutant leads to a protein with 42% comparative reactivity. The crystal structure (Fig. 6) demonstrates graphically the differential interaction of the isoleucine and tryptophan side chains with the pteridine molecule. It is interesting to note also that, although not a direct measure of affinity, the  $K_m$  value of the pteridine substrate rises to 70 μM, a figure that is 2.5 times the wild-type figure, reinforcing the concept that this mutant enzyme is less efficient in its pteridine reductive capacity. Clearly Trp<sup>86</sup> plays a significant role in creating the correct contours for the ternary complex active site.

The Ala<sup>133</sup> → Ser mutant is an interesting variant. The serine substitution is present in a majority of the known short chain dehydrogenases (7, 11) and the UDP-epimerase (34). With dihydropteridine reductase, when this substitution is made, little alteration in kinetic properties relative to wild type are observed. Although Ser<sup>133</sup> hydrogen bonds to two backbone nitrogens (Fig. 7), it is apparent that the hydroxyl group of Ser<sup>133</sup> can impinge on the active site. The position of Ser<sup>133</sup> in Ala<sup>133</sup> → Ser is consistent with the position of Ser<sup>139</sup> in 3α,20β-hydroxysteroid dehydrogenase (28). In the case of the dihydropteridine reductase reaction the availability of yet another proton source is unnecessary; however, in the case of the dehydrogenases where a proton sink is required, this serine molecule and its hydrogen bonding network may play an important role in facilitating proton transfer and thus aid the overall oxidative dehydrogenation that occurs in many

of these reactions.

It is apparent from these results that the dihydropteridine reductase dimer is very sensitive to the correctly oriented binding of the reduced dinucleotide cofactor. In particular the associations of Asp<sup>37</sup>, Lys<sup>150</sup>, and Asn<sup>186</sup> are prerequisites for a functional enzyme. Moreover, without dinucleotide present the protein rapidly loses its active conformation as is observed by the irreversible loss of activity during purification and dialysis. It is probable that a protonated Lys<sup>150</sup> is also important for the rapid elimination of NAD<sup>+</sup> after reduction has occurred. Such a function can be inferred from the NMR experiments carried out with the analogous epimerases (8), where a polarization of the nicotinamide positive charge throughout this region of the oxidized dinucleotide is observed in suitably <sup>15</sup>N-labeled NAD<sup>+</sup> derivatives. Based on the extensive hydrogen bonds around Lys<sup>150</sup>, it will undoubtedly be charged in dihydropteridine reductase and most probably in the steroid dehydrogenases where similar configurations have been reported (28, 35). The  $\epsilon$ -amino group of Lys<sup>150</sup> in dihydropteridine reductase protonated at the pH optimum of the reaction will thus diminish a potential charge-charge interaction by the ejection of NAD<sup>+</sup> after reduction of substrate has occurred. The  $K_d$  for NAD<sup>+</sup> by the wild-type enzyme is  $\sim 200 \mu\text{M}$ , demonstrating the enzyme's low affinity for the oxidized form of the dinucleotide. Because of the instability of the Lys<sup>150</sup> and Asn<sup>186</sup> mutants, particularly in the absence of cofactor, it has not yet been possible to measure the  $K_d$  values of NAD<sup>+</sup> with these mutant enzymes. The point of attachment via Asn<sup>186</sup>, where hydrogen bonding secures the carboxamide substituent of the nicotinamide and ensures the correct orientation of the pro-S hydrogen of NADH toward the incoming pteridine, gives rise to the classification of dihydropteridine reductase as a B-stereospecific dehydrogenase (36). With a mutation at 186 from asparagine to alanine, the nicotinamide portion of the NADH cannot be rigidly orientated for proper reduction of the substrate.

The mechanistically important function of Lys<sup>150</sup> to activate Tyr<sup>146</sup> is clearly lost in all the mutants occurring at both the 146 and 150 positions as is evidenced by the markedly lower  $k_{\text{cat}}$  values exhibited by these mutants. The most extreme changes occur with Tyr<sup>146</sup>  $\rightarrow$  Phe and Tyr<sup>146</sup>  $\rightarrow$  His. The compensatory positioning of water molecules in the vicinity of the substrate and the possibility that protonation could occur at the 2-, 3-, or 4-position of the quinonoid pteridine, described above, could explain, however, the residual activity observed with these mutants.

Clearly, until NADH is bound, no active site exists with this enzyme, which supports the ordered kinetics reported by previous workers (37). Of considerable importance toward completing the creation of this site is Trp<sup>86</sup>. It allows a planar aperture to form in the molecule that accommodates the sandwiching of the quinonoid dihydropteridine substrate at the site thus holding the molecule during the reductive process. After reaction the enzyme then rapidly ejects both product and NAD<sup>+</sup> and prepares for a further cycle. The instability of the

protein minus dinucleotide suggests that if intracellular concentrations of the reduced dinucleotide are low the enzyme will have a short half-life. This will be particularly so if mutations are present at positions 37, 150, or 186.

#### REFERENCES

- Nagatsu, T., Levitt, M., and Udenfriend, S. (1964) *J. Biol. Chem.* **239**, 2910–2917
- Shiman, R. (1985) in *Folates and Pterins* (Blakley, R. L., and Benkovic, S. J., eds) Vol. 2, pp. 179–249, Wiley Interscience, New York
- Kaufman, S., and Kaufman, E. E. (1985) in *Folates and Pterins* (Blakley, R. L., and Benkovic, S. J., eds) Vol. 2, pp. 251–352, Wiley Interscience, New York
- Kuhn, D. M., and Lovenberg, W. (1985) in *Folates and Pterins* (Blakley, R. L., and Benkovic, S. J., eds) Vol. 2, pp. 353–382, Wiley Interscience, New York
- Varughese, K. I., Skinner, M. M., Whiteley, J. M., Matthews, D. A., and Xuong, N. H. (1992) *Proc. Natl. Acad. Sci. U. S. A.* **89**, 6080–6084
- Su, Y., Varughese, K. I., Xuong, N. H., Bray, T. L., Roche, D. J., and Whiteley, J. M. (1993) *J. Biol. Chem.* **268**, 26836–26841
- Jörnvall, H., Persson, B., Krook, M., Atrian, S., González-Duarte, R., Jeffery, J., and Ghosh, D. (1995) *Biochemistry* **34**, 6003–6013
- Burke, J. R., and Frey, P. A. (1993) *Biochemistry* **32**, 13220–13230
- Swanson, B. A., and Frey, P. A. (1993) *Biochemistry* **32**, 13231–13236
- Varughese, K. I., Xuong, N. H., Kiefer, P. M., Matthews, D. A., and Whiteley, J. M. (1994) *Proc. Natl. Acad. Sci. U. S. A.* **91**, 5582–5586
- Persson, B., Krook, M., and Jörnvall, H. (1991) *Eur. J. Biochem.* **200**, 537–543
- Matthews, D. A., Varughese, K. I., Skinner, M., Xuong, N. H., Hoch, J., Trach, K., Schneider, M., Bray, T., and Whiteley, J. M. (1991) *Arch. Biochem. Biophys.* **287**, 234–239
- Maniatis, T., Fritsch, E. F., and Sambrook, J. (1982) *Molecular Cloning: A Laboratory Manual*, Cold Spring Harbor Laboratory, Cold Spring Harbor, NY
- Hanahan, D. (1983) *J. Mol. Biol.* **166**, 557–580
- Fromm, M., and Berg, P. (1983) *J. Mol. Appl. Genet.* **1**, 457–481
- Kunkel, T. A. (1985) *Proc. Natl. Acad. Sci. U. S. A.* **82**, 488–492
- Kunkel, T. A., Roberts, J. D., and Zabor, R. A. (1987) *Methods Enzymology* **156**, 367–382
- Webber, S., Deits, T. L., Snyder, W. R., and Whiteley, J. M. (1978) *Anal. Biochem.* **84**, 491–503
- Bradford, M. M. (1976) *Anal. Biochem.* **72**, 248–254
- Matthews, D. A., Webber, S., and Whiteley, J. M. (1986) *J. Biol. Chem.* **261**, 3891–3893
- Xuong, N. H., Sullivan, D., Neilson, C., and Hamlin, R. (1985) *Acta Crystallogr.* **B41**, 267–269
- Brunker, A. T. (1987) *X-PLOR V. 3.1. A System for X-ray Crystallography and NMR*, Yale University Press, New Haven, CT
- Jones, T. A. (1978) *J. Appl. Crystallogr.* **11**, 268–272
- Karplus, P. A., and Schulz, G. E. (1989) *J. Mol. Biol.* **210**, 163–180
- Bystroff, C., Oatley, S. J., and Kraut, J. (1990) *Biochemistry* **29**, 3263–3277
- Kim, Y., and Kreevoy, M. M. (1992) *J. Am. Chem. Soc.* **114**, 7116–7123
- Grimshaw, C. E., Matthews, D. A., Varughese, K. I., Skinner, M., Xuong, N. H., Bray, T., Hoch, J., and Whiteley, J. M. (1992) *J. Biol. Chem.* **267**, 15334–15339
- Ghosh, D., Wawrzak, Z., Weeks, C. M., Duax, W. L., and Erman, M. (1994) *Structure* **2**, 629–640
- Armarego, W. L. F. (1979) *Biochem. Biophys. Res. Commun.* **89**, 246–249
- Armarego, W. L. F., and Waring, P. (1982) *J. Chem. Soc. Perkin Trans. II* **21**, 1227–1233
- Bohren, K. M., Grimshaw, C. E., Lai, C.-J., Harrison, D. H., Ringe, D., Petsko, G. A., and Gabbay, K. H. (1994) *Biochemistry* **33**, 2021–2032
- Ribas de Pouplana, L., and Fothergill-Gilmore, L. A. (1994) *Biochemistry* **33**, 7047–7055
- Benkovic, S. J., Sammons, D., Armarego, W. L. F., Waring, P., and Inners, R. (1985) *J. Am. Chem. Soc.* **107**, 3706–3712
- Bauer, A. J., Rayment, I., Frey, P. A., and Holden, H. M. (1992) *Proteins Struct. Funct. Genet.* **12**, 372–381
- Ghosh, D., Pletnev, V. Z., Zhu, D. W., Wawrzak, Z., Duax, W. L., Pangborn, W., Labrie, F., and Lin, S. X. (1994) *Structure* **3**, 503–513
- You, K.-S. (1985) *CRC Crit. Rev. Biochem.* **17**, 313–451
- Korri, K. K., Chippel, D., Chauvin, M. M., Tirpak, A., and Scrimgeour, K. G. (1977) *Can. J. Biochem.* **55**, 1145–1152
- Shahbaz, M., Hoch, J. A., Trach, K. A., Hural, J. A., Webber, S., and Whiteley, J. M. (1987) *J. Biol. Chem.* **262**, 16412–16416